



# Investigation on esterified pectin as natural hydrate inhibitor on methane hydrate formation

Adam Daniel Effendi<sup>1</sup> · Chee Wee Sia<sup>1</sup> · Mazuin Jasamai<sup>1</sup> · Muhammad Asad Hashmani<sup>1</sup>

Received: 21 October 2021 / Accepted: 20 March 2022 / Published online: 11 April 2022  
© The Author(s) 2022

## Abstract

Flow assurance treatment with chemical have become more common as new natural polymers are being develop and are viable for inhibiting hydrate formation in production systems due to its eco-friendly and economical properties. Using high-pressure micro-differential scanning calorimetry (HP- $\mu$ DSC), the influence of kinetic inhibition on methane gas hydrate formation from synthetic polymer; polycaprolactam (PVCap) and organic polymers (low- and high-methoxylated pectin) was investigated. HP- $\mu$ DSC was combined with the use of open-ended capillary tubes to counter the stochasticity of hydrate formation which often results in an inconclusive data set without numerous repetitions. By adding the capillary tubes within the cell, more data points on the performance of the inhibitors. Generally, the addition of these inhibitors increased the delay in formation of hydrates compared to the control sample which contained deionized water at 25°C subcooling and 10 MPa pressure. However, the two types of organic inhibitors, which are distinguished primarily by the functional group ratios (carboxyl and ester), performed in contrast to one another. The results suggest that the presence of higher carboxyl functional groups is affecting the overall polarity (i.e., low-methoxylated pectin) significantly improved the hydrate inhibition at optimum concentration where both high-methoxylated pectin and PVCap; a commercial inhibitor, performed relatively weaker. In comparison with PVCap, high-methoxylated pectin showed comparable trend and slightly better performances at most concentrations; however, the peak structures indicate discernible difference in the formation mechanism. The use of low-methoxylated pectin at optimum concentration may offer inhibition performance up to three times to that of PVCap at high subcooling.

**Keywords** Polysaccharide · Low- and high-methoxylated pectin · Gas hydrates · Induction time · High-pressure micro-differential scanning calorimetry

## Introduction

Hydrate formation is one of the most prominent problems under flow assurance. Hydrate formation occurs where the pressure is high, or the temperature is very low; and these factors are interdependent (Makogon 2019). This means

that in major oil and gas producing countries including Canada, Russia and the USA, where surface temperatures could drop below freezing temperature, hydrate formation mitigation plan is considered to maintain year-round production. Furthermore, hydrate mitigation becomes more vital as the sector moves toward deep-water and arctic production, where operational expenditures and conditions can be high and extreme, respectively (Makwashi et al. 2018). Conventional methods to control hydrate formation involve the use of glycol or methanol which are classified as thermodynamic hydrate inhibitors (THI). These THIs are used in massive quantities ranging from 30 to 60 wt%, through which the hydrate equilibrium is shifted away from the system operating profile. This makes them expensive and logistically inconvenient to be applied, especially in extreme and remote regions. Another issue stemming from THIs is pollution, which might develop if efficient regeneration

✉ Adam Daniel Effendi  
adam\_20001972@utp.edu.my

Chee Wee Sia  
sia\_cheewee@utp.edu.my

Mazuin Jasamai  
mazuin\_jasamai@utp.edu.my

Muhammad Asad Hashmani  
asad.h\_22222@utp.edu.my

<sup>1</sup> Department of Petroleum Engineering, Universiti Teknologi PETRONAS, Seri Iskandar, Malaysia

facilities are not used. In the last 20 years, oil and gas industry has been seeking alternative solutions using low-dosage hydrate inhibitors (LDHIs) which consists of two primary types of inhibitors: kinetic hydrate inhibitors (KHIs) and anti-agglomerants (AAs). As the name suggests, LDHIs are used in minute quantities ranging from 0.1 to 3.0 wt.% (Kelland 2016, 2018; Wang et al. 2019; S. Xu, et al. 2016a, b). Initially, the successful synthetic polymers under KHI class such as polyvinylpyrrolidone (PVP) and polycaprolactum (PVCap) were applied to mitigate hydrate formation. Although they may be inexpensive when compared to the use of thermodynamic inhibitors, these synthetic polymers still raise an environmental concern due to its toxicity and the inability to biodegrade (Kelland 2018). As a result, this problem statement encourages the industry to develop green LDHIs solutions that improve performance without harming the environment.

In the last decade, several biofriendly kinetic hydrate inhibitors have been researched to identify their potential such as polysaccharides (starch, pectin, cellulose, chitosan) and proteins (Yaqub, bin Mohd Shariff, Mellon 2019; Silva et al.; Kamal et al. 2016; P. Xu et al. 2016a, b; Daraboina, Malmos Perfeldt and von Solms 2015; Y. Xu, Yang, Yang 2010). These studies have yielded encouraging findings, but the mechanism and impact of molecular structure and functional group composition have yet been determined.

Properties that have been related to inhibitors' performance include operating pressure (Semenov et al. 2015), subcooling (Semenov et al. 2015), hydrophobicity (Baek et al. 2018; Sa et al. 2013), carbon chain length (Gupta and Sangwai 2017), molecular weight (Li et al. 2020; Farhadian and Varfolomeev 2019), gas composition (Tohidi, Anderson, Tohidi 2018) and water salinity (Jiménez-Ángeles and Firoozabadi 2018).

In this research, hydrophobicity due to the functional group is used to explained the different performance of the pectin. So far, the general interaction of hydrophobic and hydrophilic groups with gas hydrate has been understood. It has been discovered that the hydrophobic effect is important in the development of gas hydrates. The dissolved hydrophobe helps to promote hydrate formation by organizing the surrounding water molecules into a hydrate structure. Hydrophile, on the other hand, disturbs the surrounding water structure by vying for water with the gas (Nguyen and Nguyen 2017). As a result, the kinetic mechanism can be viewed as adsorption or perturbation similar to amino acid inhibition mechanism (Sa et al. 2014, 2013). Both mechanisms would occur during the inhibition in both experiments and on the field. Therefore, a natural polymer that has inhibitory property as well able to influence its hydrophobicity through influencing its functional group was chosen which is pectin also known as pectic polysaccharide. Pectin which is normally present in most plant parts, even in the peels

and seeds of the fruits and vegetables which are normally considered a waste product (Vanitha and Khan 2019). This makes pectin, because of its abundance, a very high potential polymer. Several researches have been performed on pectin obtained from different sources (calamansi peels, citrus peels, etc.) which show favorable results as kinetic hydrate inhibitor (Idress et al. 2019; S. Xu, et al. 2016a, b). Yet, despite the amount of research performed on pectin, specific study on the different classes of pectin has not been performed. Considering that pectin can be divided into two main categories, i.e., high-methoxylated pectin (HMP), which has a degree of esterification (%DE) higher than 50% (greater than 50% ester to carboxyl ratio) and low-methoxylated pectin (LMP) which has less than 50% degree of esterification (lesser than 50% carboxyl to ester ratio) (Sriamornsak 2003), it is important to identify which one of these categories is more suited to be used as hydrate inhibitor. Furthermore, pectin can be chemically modified to support its function as kinetic hydrate inhibitor (Chen et al. 2015). Therefore, this study starts base by representing two major classes of pectin which can lead to new potential hydrate inhibitor candidates.

Although high-pressure micro-differential scanning calorimetry (HP- $\mu$ DSC) used may not be reflective of field conditions due to its static nature, it could still provide insight into its limit as the fluid flow regime in the pipeline encourages hydrate growth, and thus the result obtained in a stagnant environment should be considered the upper bound of delaying hydrate growth (Maeda et al. 2018). Due to the stochastic nature of hydrate formation, which can necessitate multiple retests before reporting, recent methodology optimization devised the use of closed-end capillary tubes (to obtain more results in a single run) and silica gel (to improve visibility of hydrate formation) with HP- $\mu$ DSC to yield more statistical results which resulted in fewer runs (Daraboina et al. 2013).

This research has used HP- $\mu$ DSC along with open-ended capillary tubes to obtain a statistical trend of hydrate inhibition performance using three different concentrations (0.10, 0.50 and 1.00wt%) of each chemical: PVCap, HMP and LMP. The experiment was conducted under isothermal temperature setting to obtain the result as a function of time (referred to as induction time) at a subcooling of 25 °C and 10 MPa pressure. This research attempts to enhance the development of green kinetic hydrate inhibitors, specifically pectin, by relating the function of molecular structure and composition of the two functional groups ( $-\text{COOH}$  and  $-\text{COOCH}_3$ ). The goal of this research is to quantify the effect of change caused by replacing one hydrophobic functional group with one hydrophilic group throughout the repeating unit of the polymer. By assessing this value, we can observe the optimum DE% and further improve the composition of pectin through several modifications that

are available for pectin. These chemical modifications can possibly improve the induction time over a higher range of operating parameters significantly while maintaining the biodegradability of the polymer.

## Materials and methods

### Materials

The two types of pectin, LMP (average degree of esterification 25–35%) and HMP (average degree of esterification 72–82%), were purchased from Henan Chemical Career Company. Synthetic KHI PVCap was purchased from Sigma-Aldrich Chemicals. Chemicals to perform titration, i.e., phenolphthalein, sodium hydroxide, hydrochloric acid and ethanol, were purchased from Sigma-Aldrich Chemicals. Capillary tubes (length 5 mm x  $\varnothing$  2 mm) were obtained from Xi De Technology Co., Ltd (Fig. 1). Deionized water used to prepare samples and methane gas for the experiments was supplied by Universiti Teknologi PETRONAS. All materials were funded by Yayasan Universiti Teknologi PETRONAS under grant 015LC0-160.

### Methodology

#### Degree of esterification

To further characterize the pectins, titration was performed on each type to precisely identify the degree of esterification using a methodology described in (Sayah et al. 2016).

A 0.25 g of pectin was soaked with 2 mL ethanol before being diluted to a 25 mL solution of water. The solution

received two drops of phenolphthalein. To neutralize the free carboxyl acids from anhydro-galacturonic acid, the titration was initiated by progressively adding 0.25 M sodium hydroxide. The volume of 0.25 M sodium hydroxide used for this process was recorded as  $V_1$ . Afterward, 10 mL of 0.25 M sodium hydroxide was added and stirred for 30 min for hydrolysis, followed by the addition of 10 mL of 0.25 M hydrochloric acid and stirring until the complete disappearance of pink color of the indicator. Hydrochloric acid excess was titrated using 0.1 M sodium hydroxide. The number of esterified carboxyl groups was calculated from the volume of 0.1 M sodium hydroxide used for the titration which was recorded as  $V_2$ . The number of esterified carboxyl groups was calculated from the volume of 0.1 M sodium hydroxide used for the titration which was recorded as  $V_2$ . The %DE of the pectin was calculated using Eq. 1.

$$\%DE = V_2 / (V_1 + V_2) \times 100\% \quad (1)$$

The procedure was triplicate to average the %DE.

#### Hydrate equilibrium test

High-pressure micro-differential scanning calorimetry Evo7 (HP- $\mu$ DSC VII Setaram, Inc.) containing two 1 cc high-pressure cells operated at 0.1 to 40 MPa and  $-45$  °C to  $+100$  °C. On separate runs, methodology using (1) deionized water bulk sample (5 $\mu$ L) and (2) four capillary tubes (length 5 mm  $\times$   $\varnothing$  2 mm) were applied. The capillary tubes were filled with 2–4 $\mu$ L of deionized water using microsyringe before transferring into the cell horizontally (to prevent the pressure from expelling the sample from the tube into the cell). Primarily, capillary tubes are used because

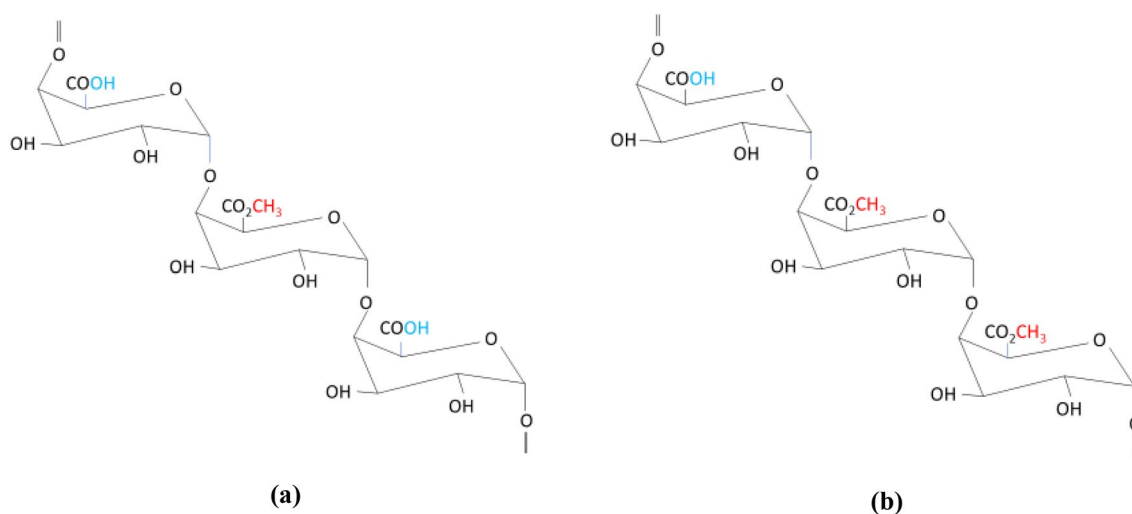


**Fig. 1** The repeating unit of pectin (homogalacturonan acid). The figure displays the major difference in the **a** low %DE and **b** high %DE pectin. The difference can be observed in the carboxyl unit of the polymer

hydrate nucleation in bulk stagnant solutions with no mixing is restricted due to mass transfer limitations which leads to ice formation (Daraboina, Malmos Perfeltd, von Solms 2015). In theory, with more surface exposure to the gas, more hydrate formation and dissociation should be observed as shown in Fig. 2(b). Hence, initial test was conducted to confirm this application when placing the capillary tube horizontally. A study done by Daraboina, Malmos Perfeltd, von Solms (2015), has shown that HP- $\mu$ DSC methodology could be modified specifically for assisting and optimizing evaluation and investigation of hydrate with HP- $\mu$ DSC.

This test was done to understand the difference in accuracy and visibility of the hydrate peaks using bulk sample and capillary tubes, while also obtaining precise value for hydrate equilibrium to set up the kinetic hydrate inhibitor performance test. HP- $\mu$ DSC was used to experimentally determine the equilibrium temperature following a pre-described temperature program (Nashed et al. 2014).

From Daraboina et al. (2013) findings, the method used are the ramping method and isothermal method. These both methods can be used complementarity to better form a methodology. Similar to (Daraboina et al. 2013), the ramping method would allow determination of equilibrium temperature for ice and hydrate formation. Also, it would allow researchers to determine the temperature where ice forms. This information lets the isothermal method to be used with reduced or completely without ice formation by putting the subcooling temperature approximately above the ice formation temperature. Difficult ice and hydration interpretation can be avoided by using this process.

It started with the cell pressurized to 10 MPa using methane gas. During the ramping method, after the desired pressure was obtained in the cell, the temperature program was initiated. In the first 30 min, the temperature was cooled down to  $-20\text{ }^{\circ}\text{C}$  using  $1.0\text{ }^{\circ}\text{C}/\text{min}$  cooling rate and held

at the temperature for 20 min to ensure formation of ice and hydrate. After the 10 min of isothermal condition, the temperature was slowly raised to  $25\text{ }^{\circ}\text{C}$  using  $0.01\text{ }^{\circ}\text{C}/\text{min}$  heating rate. This method of determining the equilibrium temperature was used based on description of equilibrium temperature in (Sloan Jr and Koh 2007). The formation peaks were observed to understand the immediate effect of capillary tubes to validate methodology and the dissociation peaks of ice and hydrate were analyzed. The results were compared with experimental data from previous study to validate the equilibrium temperature (Gayet et al. 2005; Sloan Jr and Koh 2007; McCain 1990).

### Kinetic hydrate inhibitor performance test

For the kinetic hydrate inhibitor performance test, isothermal temperature program was selected to visualize discrete nucleation events at 10 MPa and the specified subcooling of  $25\text{ }^{\circ}\text{C}$ . In terms of subcooling, Del Villano, Kommedal and Kelland (2008) stated that current KHIs (commercial) applications offshore are limited to a  $\Delta T$  subcooling maximum of about  $10\text{--}12\text{ }^{\circ}\text{C}$ . However, for experimentation, evaluation can be done at higher subcooling to further encourage the formation to occur to reduce time taken for each run and the use of new inhibitor may allow application at higher subcooling. Once the hydrate equilibrium was established, the isothermal temperature was calculated using Eq. 2.

$$\text{Isothermal temperature} = \text{Equilibrium Temperature} - \text{Subcooling Temperature} \quad (2)$$

Using methodology from Daraboina et al. (Daraboina, Malmos Perfeltd, von Solms 2015; Daraboina et al. 2013) with slight modifications, for the isothermal method, the four capillary tubes placed inside the cell sample were

**Fig. 2** **a** Conventional HP- $\mu$ DSC sample (bulk). **b** Four open-ended borosilicate tubes are placed horizontally inside the HP- $\mu$ DSC cell to promote hydrate formation

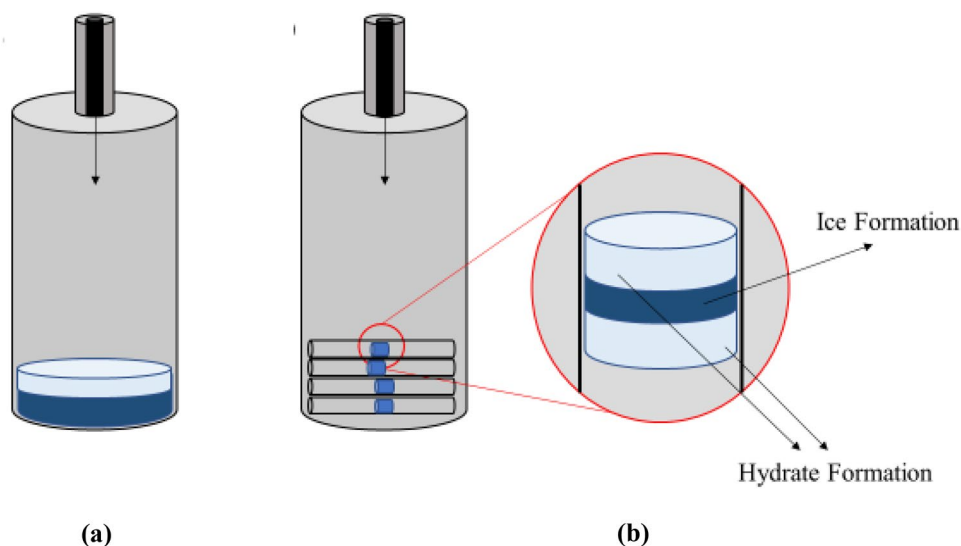




**Fig. 3** Capillary Tubes containing sample placed inside the HP-μDSC cell

pressurized to 10 MPa cooled at 1 °C/min to isothermal temperature, held constant (7 h for pure water sample and 12 h for inhibitor samples) and reheated back to 20 °C at the heating rate of 1 °C/minute (Fig 3). Unlike from some referenced literature (Daraboina et al. 2011; Gayet et al. 2005), silica gel was not used in this experiment and instead of closed-end, open-ended capillary tubes were used.

With entire focus on hydrate inhibition, deionized water (DW) and three different concentrations (0.1, 0.5 and 1.0 wt%) of each chemical (LMP, HMP and PVCap) were tested three times each. A fresh sample was used each time to avoid memory effect (Rogers 2015). Due to the separation of sample within the cell, more nucleation events were captured which allowed the observation of trend in data with fewer runs.

### Analysis

After obtaining the data from HP-μDSC for kinetic hydrate inhibition performance test, the onset time was noted for each peak. The nucleation time was calculated as shown in Eq. 3.

$$\text{Nucleation Time} = \text{Peak Onset Time} - \text{Equilibrium Time} \quad (3)$$

where equilibrium time is:

$$\text{Equilibrium Time} = (\text{Initial Temperature} - \text{Equilibrium Temperature}) \times (\text{Cooling Rate}) \quad (4)$$

**Table 1** Results obtained from titration

Pectin type	Test	V1	V2	%DE	Average %DE	Standard deviation
LMP	1	2.70	1.00	27.03	24.34	± 2.51
	2	3.20	0.85	20.99		
	3	2.40	0.80	25.00		
HMP	1	0.80	2.20	73.33	74.99	± 1.54
	2	0.80	2.35	74.60		
	3	0.70	2.35	77.05		

The nucleation time of all the peaks was accounted for and averaged to obtain an average nucleation time for each run.

$$\text{Average Nucleation Time} = (\text{NT}_1 + \text{NT}_2 + \dots + \text{NT}_n) / n \quad (5)$$

where NT refers to the nucleation time.

Once the average nucleation time for all three runs was obtained, the average nucleation times from all three runs were further averaged to obtain the induction time for the sample.

$$\text{Induction Time} = (\text{ANT}_1 + \text{ANT}_2 + \text{ANT}_3) / 3 \quad (6)$$

where ANT refers to the average nucleation time.

Finally, the relative inhibitor performance (RIP) was calculated using the formula as described in previous research (Yaqub et al. 2018).

$$\text{RIP} = (\text{Induction Time}_{\text{sample}} - \text{Induction Time}_{\text{water}}) / \text{Induction Time}_{\text{water}} \quad (7)$$

## Results

### Degree of esterification

The degree of esterification was provided by the supplier in a range of ± 15%. Using the titration method, %DE of each pectin was experimentally measured precisely. With this significant difference in %DE, the impact of functional group ratio (ester: carboxyl) can be studied clearly. Quite evidently, LMP holds more carboxyl functional group and lower ester and vice versa for HMP. Table 1.

### Hydrate equilibrium test

Hydrate formation during the equilibrium test was scanned to see the immediate effect of using the capillary tubes. As observed in Fig. 4, twice as many nucleation peaks were present in the test using capillary tubes. The two different detectable heat-flow signals in both samples show ice and hydrate formation which can also be correlated to the dissociation.

**Fig. 4** Hydrate formation using bulk and capillary tube samples in HP- $\mu$ DSC. The energy absorbed in the dissociation was also considered, which is reflective of the amount of ice and hydrate melting.

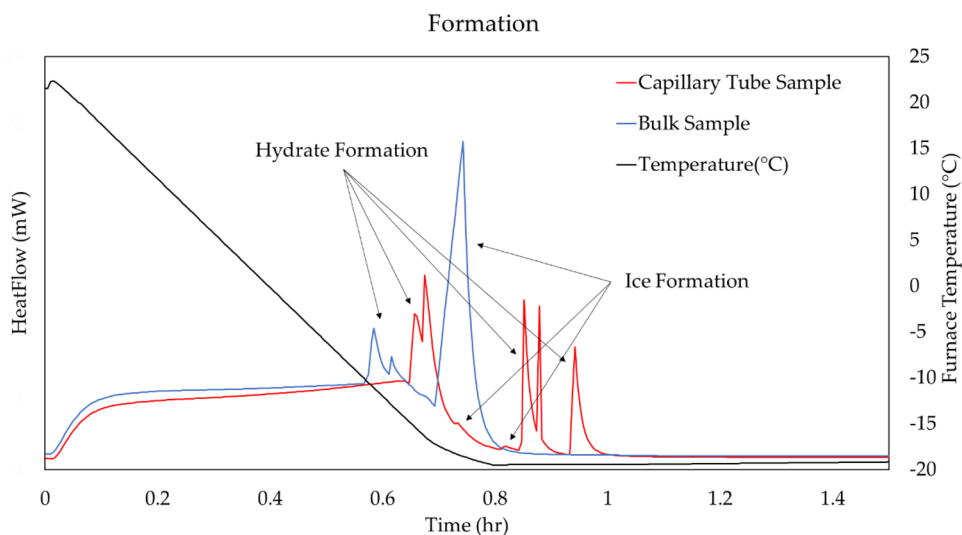
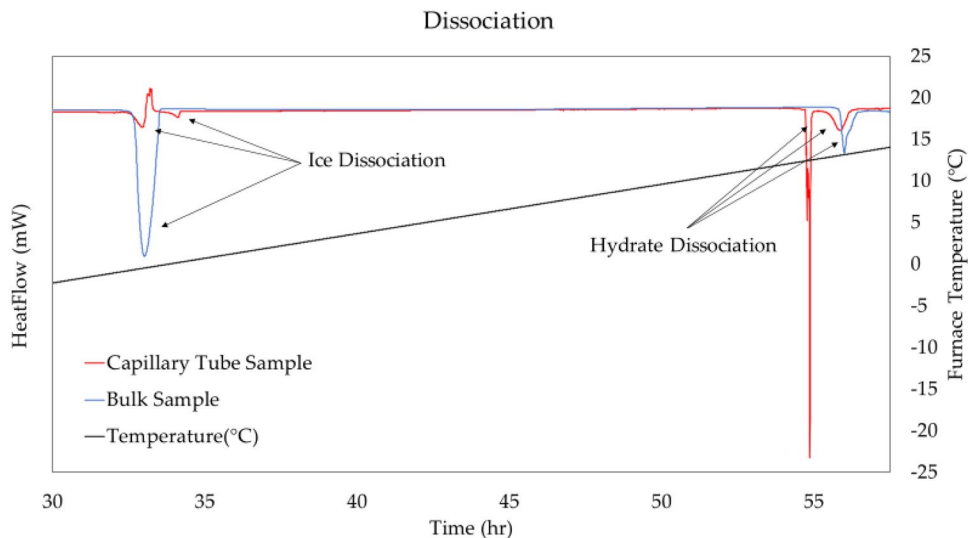


**Fig. 5** Hydrate dissociation using bulk and capillary tube samples in HP- $\mu$ DSC



With bulk sample, ice formation heat-flow signal was nearly three times as strong reducing the visibility of the hydrate formation signal. Using capillary tubes, only a portion of the massive ice formation occurred, and the remaining three peaks submit the value of hydrate nucleation events.

In bulk sample, a massive ice melting compared to hydrate melting is observed, whereas, in capillary tube sample four times as much energy were absorbed during hydrate dissociation as compared to ice. As dissociation of hydrates displays less stochasticity, it can be safely assumed that in terms of accuracy, capillary tubes reported a more precise equilibrium temperature compared to bulk sample. In terms of visibility of hydrate formation and dissociation, peaks became significantly more visible using capillary tubes. Therefore, the methodology using capillary tube for kinetic hydrate inhibition performance test is clearly identified to be better and was used for evaluating LMP (Fig. 5),

HMP and PVCap performance. Data obtained from ice and hydrate dissociation peaks for both runs are tabulated below (Table 2):

To further confirm the result obtained is viable, utilizing hydrate formation phase diagram from McCain (1990) as shown in Fig. 6. Additionally, through the ramping method, several runs were also done to confirm the equilibrium temperature following the set experiment condition (100 MPa and temperature below  $-8^{\circ}\text{C}$ ). Through this method, the approximate ice nucleation temperature was determined to be approximately at  $-13.52^{\circ}\text{C}$  and  $-11.40^{\circ}\text{C}$  for tube and bulk sample, respectively. This result is within expectation for bulk samples; ice nucleation is easier and has a higher tendency to form when compared to using capillary tubing where hydrate nucleation should form easily due to larger surface area of the fluid exposed. Also, to note that, when ice nucleation occurs, it would take the water required to

**Table 2** Results obtained from dissociation of tube and bulk samples

Sample Type	Ice dissociation temperature <sup>1</sup> (°C)	Hydrate dissociation temperature <sup>1</sup> (°C)	Error <sup>2</sup> (%)	Ice dissociation energy (J)	Hydrate dissociation energy (J)	Ice to hydrate ratio
Bulk Sample	-0.672	13.059	4.81	$1.62 \times 10^6$	$3.49 \times 10^5$	4.642
Tube Sample	-0.345	12.658	1.59	$6.97 \times 10^5$	$2.613 \times 10^6$	0.267

<sup>1</sup>Onset for both ice and hydrate peaks in the run with capillary tubes were averaged to obtain a singular value for dissociation temperature of each

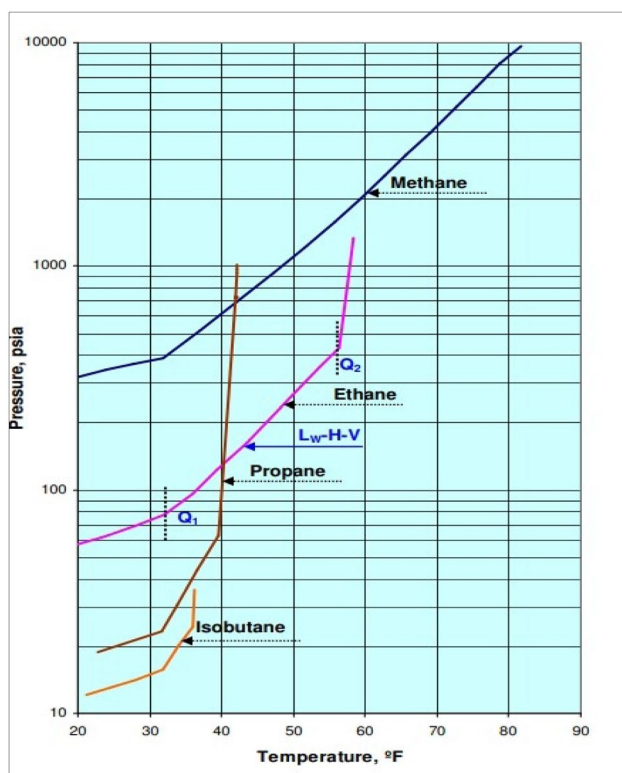
<sup>2</sup>The error% was calculated with respect to experimental results on methane hydrate equilibrium reported in previous study. (Gayet et al. 2005)

form hydrate, thus lowering the amount of hydrate nucleation which is something that should be avoided.

From Fig. 6, it is approximately at 12.78 °C ~ 13°C (55°F) in which hydrate would start to form when only methane gas is present during cooling at 10 MPa. As a result, after comparing the acquired findings (Table 3), it is determined to be within appropriate range. After determination of the equilibrium temperature, isothermal temperature for kinetic hydrate inhibitor performance test was calculated using Eq. 2.

Isothermal Temperature

$$= 13.432 \text{ °C} - 25 \text{ °C} = -11.568 \text{ °C} \approx -12 \text{ °C}$$

**Fig. 6** Hydrate Formation Phase Diagram (McCain 1990)

$$\text{Isothermal Temperature} = 13.432 \text{ °C} - 25 \text{ °C} = -11.568 \text{ °C} \approx -12 \text{ °C}$$

The isothermal temperature would be set at -12°C which is above the approximate ice nucleation. Therefore, during the isothermal method, it is expected that ice nucleation would not occur or at least reduced similarly to methodology conducted by Daraboina et al. (2013).

## Kinetic hydrate inhibitor performance test

### Deionized water (DW)

To be able to calculate the relative inhibition power, the performance testing was initiated with water samples without any inhibitor. Obtained charts are plotted in Fig. 7.

With time taken to reach the hydrate equilibrium in account, nucleation events were captured mainly between 30 and 180 min without any inhibitor. The earliest peak was observed at 36.66 min while the latest peak was noted at 152.89 min. Nucleation without any inhibitor displayed nucleation peaks within a narrow time range, with a standard deviation of only 37.48 min. The data are tabulated in Table 4, and the induction time is reported as shown below.

### Polycaprolactum (PVCap)

Testing the industrial kinetic hydrate inhibitor, PVCap, allows benchmarking the performance of the proposed inhibitors, HMP and LMP. As PVCap has shown better performance under high subcooling in experimental studies (Kang et al. 2014), it was chosen over PVP to standardize this test. Although three runs were performed for each concentration, the most representative runs are plotted in Fig. 8. Results for all three trials for the three concentrations of PVCap are shown in Fig. 13, 14, 15.

Using PVCap at 0.1 and 1.0 wt% yielded nearly similar results, unlike PVCap at 0.5 wt% where a significant part of hydrate formation was observed before 90 min. The first nucleation time (from all three repetitions) was observed at 45.54, 36.90 and 57.66 min for 0.1, 0.5 and 1.0 wt%, respectively. Higher variation in peak structures was observed using PVCap where, unlike HMP and LMP, broad peaks

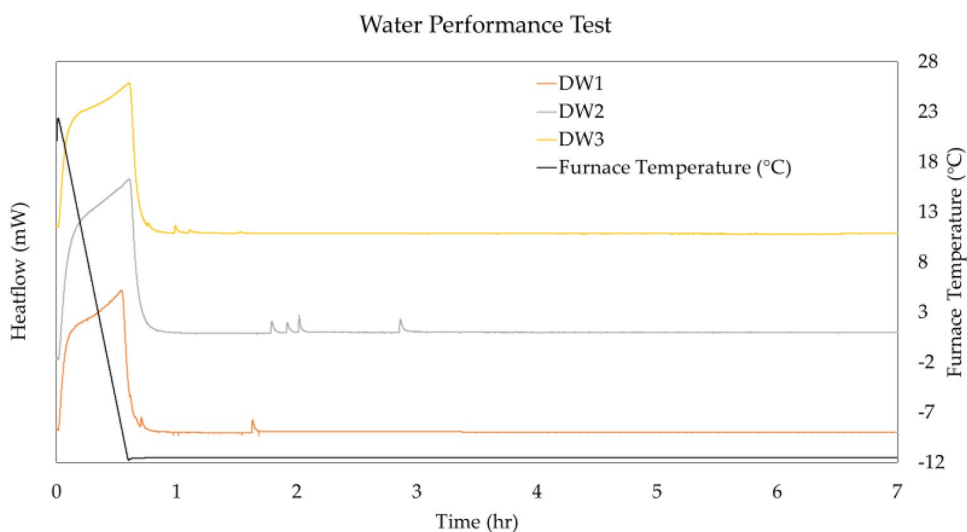
**Table 3** Equilibrium temperature of ice and hydrate

Condition set	Average ice equilibrium temperature (°C)	Average hydrate equilibrium temperature (°C)
100 Bar (10 MPa) – High Sub Cooling (Temperature below – 8°C)	– 0.0697 ~ 0	13.423 ~ 13

were also observed indicating nucleation events occurring over a slower rate of formation. Similar feature of PVCap was also captured in other previous research, where it is

described as two-phase hydrate inhibition. The phase one being disruption (perturbation) of water rings using hydrophilic functionality of the polymer, and phase two being adsorption of PVCap onto the face of the water cage attributed to the hydrogen bonding and the hydrophobic part of PVCap (Liu et al. 2020). Analysis of results from all the runs is summarized in Table 5.

Taking in account of the first peaks and the calculated induction time, it can be safely assumed that the weakest performance using PVCap was noticed at 0.50 wt%. The data spread also indicate that the spread of nucleation peaks using 0.50 wt% is not wide as compared to 0.10 or 1.00 wt%.

**Fig. 7** Data obtained from HP- $\mu$ DSC without using any inhibitor**Table 4** Results analyzed from KHI performance test in absence of kinetic hydrate inhibitor at 10 MPa and 25 °C subcooling

Sample name	Peak onset time (hr)	Peak onset time (min)	Nucleation Time <sup>a</sup> (min)	Average nucleation time (min)	Induction time (min)	Standard deviation <sup>b</sup> (min)
DW1	0.611	36.66	26.10	43.28	72.34	± 37.48
	0.653	39.18	28.62			
	0.699	41.94	31.38			
	1.626	97.56	87.00			
DW2	1.590	95.43	84.87	104.12		
	1.709	102.54	91.98			
	1.798	107.87	97.31			
	2.548	152.89	142.33			
DW3	0.676	40.55	29.99	69.61		
	0.876	52.53	41.97			
	0.984	59.05	48.49			
	1.362	81.71	71.15			
	1.676	100.56	90.00			
	2.444	146.64	136.08			

<sup>a</sup>Equilibrium Time was calculated to be 10.56 min using Eq. 4

<sup>b</sup>Standard deviation was calculated using Nucleation Time of all runs altogether



**Fig. 8** Data obtained from HP- $\mu$ DSC for KHI performance test using 0.10–1.00wt.% PVCap

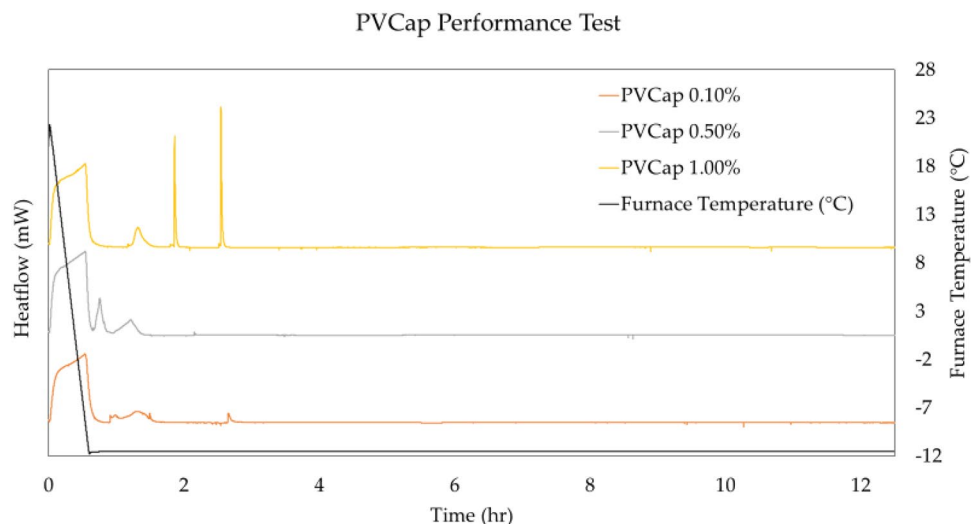


**Table 5** Induction time obtained from testing 0.10–1.00wt% PVCap at 10 MPa and 25 °C subcooling

Sample	Run	Average nucleation time (mins)	Induction time (mins)	Standard deviation (mins)	Relative inhibitor performance (RIP)
PVCap 0.10wt %	1	98.43	143.69	137.56	0.97
	2	249.90			
	3	82.73			
PVCap 0.50wt%	1	133.56	104.07	93.22	0.44
	2	111.65			
	3	67.00			
PVCap 1.00wt %	1	100.66	149.12	122.88	1.06
	2	257.31			
	3	89.40			

### High-methoxylated pectin (HMP)

Like PVCap, HMP yielded poor results at 0.50 wt% sample, whereas the 0.10 wt% and 1.00 wt% samples statistically displayed better performance for HMP as shown in Fig. 9. Results for all three trials for the three concentrations of HMP are shown in Fig. 16–18.

The earliest nucleation for each sample was observed at 20.4, 27.6 and 27.3 min for 0.10, 0.50 and 1.00wt%, respectively, while the latest nucleation for each sample was observed at 395.20, 540.24 and 399.42 min. Even though HMP 0.50 wt% displayed better performance on one of the three trials, the other two runs displayed peaks in a narrow range between 30 and 150 min. Analysis of results from all the runs is summarized in Table 6.

Even though relatively much higher performance was expected from HMP compared to PVCap, results displayed

nearly identical performances. This means that HMP, like PVCap, due to its high methyl esterification ( $-\text{CH}_3$ ) or hydrophobicity, does not inhibit methane hydrate well. Nonetheless, the poor performance of PVCap could also be related to the structural difference in the repeating units of the polymer.

### Low-methoxylated pectin (LMP)

As shown in Sect. 3.1, with a 25% DE, LMP technically has 50% more carboxyl functional groups than HMP (75% DE). This means LMP has a higher potential to attract water and gas molecules. With 0.10 wt% LMP the earliest peak observed was at as 7.14 min while the latest peak was observed at 162.72 min, which indicates at 0.10 wt% LMP performance was as good as inhibition without any inhibitor. For 0.50 and 1.00 wt% LMP, nucleation as quick as

**Fig. 9** Data obtained from HP- $\mu$ DSC for KHI performance test using 0.10–1.00wt.% HMP

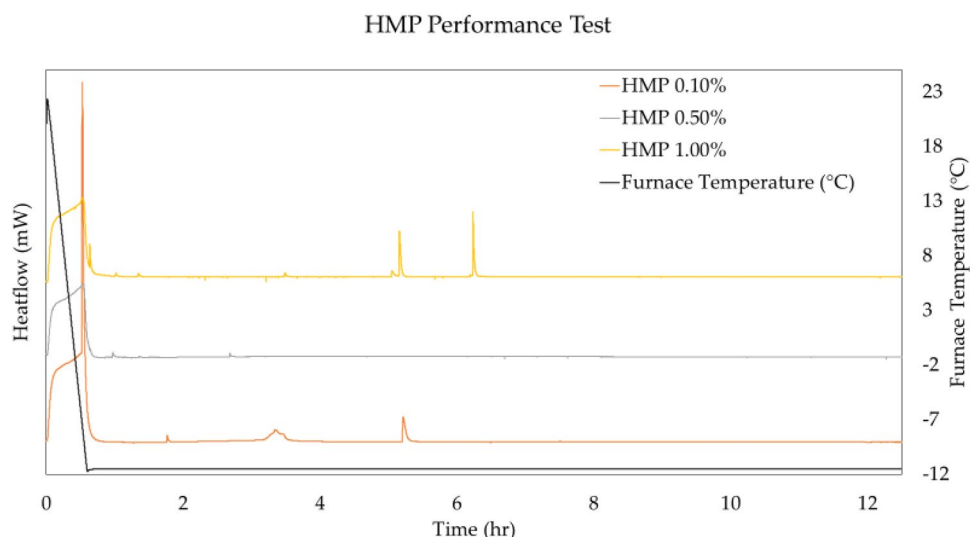


**Table 6** Induction Time obtained from testing 0.10–1.00wt% HMP at 10 MPa and 25 °C subcooling

Sample	Run	Average nucleation time (mins)	Induction time (mins)	Standard deviation (mins)	Relative inhibitor performance (RIP)
HMP 0.10wt %	1	196.25	134.07	118.73	0.80
	2	150.80			
	3	55.16			
HMP 0.50wt%	1	226.14	115.86	136.61	0.67
	2	62.688			
	3	58.752			
HMP 1.00wt%	1	228.87	156.35	134.45	1.16
	2	185.02			
	3	55.16			

29.40 min and 26.16 min was observed, although the last nucleation peak was observed just as late at 681.96 min and 620.10 min, respectively. Collectively LMP 1.00 wt% performance was as good as PVCap or HMP at 0.50 wt%. Formation peaks were generally in a narrow time scale for both 0.10 and 1.00 wt%. However, LMP 0.50 wt% displayed outstanding performance in all three runs showing, both, average nucleation times and induction time above 200 min. Results for all three trials for the three concentrations of LMP are shown in Fig. 19–21. Representative runs of each concentration for LMP are plotted in Fig. 10.

Data obtained from HP- $\mu$ DSC for all the LMP runs are summarized in Table 7. The calculated induction time and relative inhibition performance agree with the conclusion drawn from the minimum and maximum nucleation peak times.

## Discussion

Figure 11 displays the nucleation times obtained from all the tests conducted in this research. Interestingly, LMP 0.5wt% displayed highest average and data scatter among all other tests conducted; however for the same chemical 0.1 and 1.0wt% illustrate mean performance even weaker than sample without any inhibitor, whereas, by comparing PVCap and HMP it is seen that both chemicals have identical performance except at 0.1wt% where PVCap outperforms HMP by 25% at its best. Slight promotion activity can be noticed by the fact that three out of nine average nucleation times from HMP were calculated to be below 0. Similarly, LMP also displayed RIP below 0 at 0.1 and 1.0wt% indicating minor hydrate promotion. Strikingly, PVCap despite having generally poor performance only promoted hydrate at 0.5wt%, the concentration where its performance is already

**Fig. 10** Data obtained from HP- $\mu$ DSC for KHI performance test using 0.10–1.00wt.% LMP

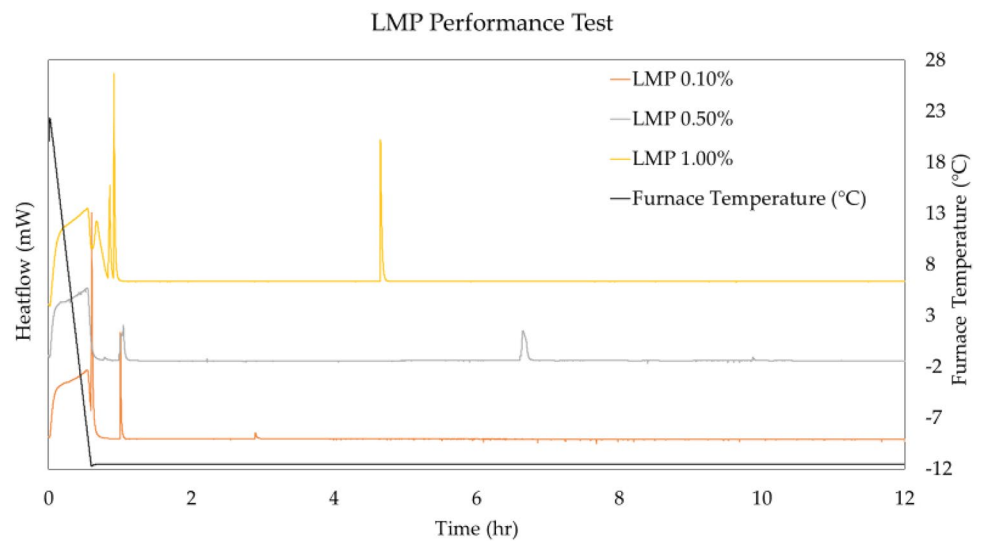


**Table 7** Induction Time obtained from testing 0.10–1.00wt% LMP at 10 MPa and 25 °C subcooling

Sample	Run	Average nucleation time (mins)	Induction time (mins)	Standard deviation (mins)	Relative inhibitor performance (RIP)
LMP 0.10wt %	1	92.87	78.48	55.75	0.08
	2	63.46			
	3	79.12			
LMP 0.50wt%	1	368.09	285.77	240.78	2.95
	2	263.18			
	3	226.06			
LMP 1.00wt%	1	95.01	102.51	157.96	0.42
	2	158.47			
	3	54.04			

**Fig. 11** Nucleation times observed from all samples Considering baseline as hydrate inhibition without any inhibitor, i.e. 0, the induction time calculated from the performance test was also converted to RIP and plotted in Fig. 12 for all the chemicals

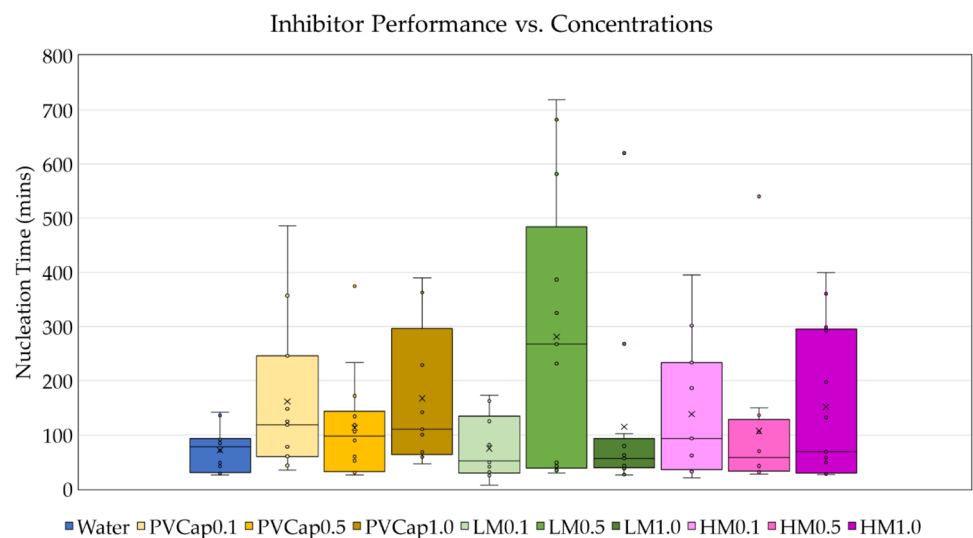
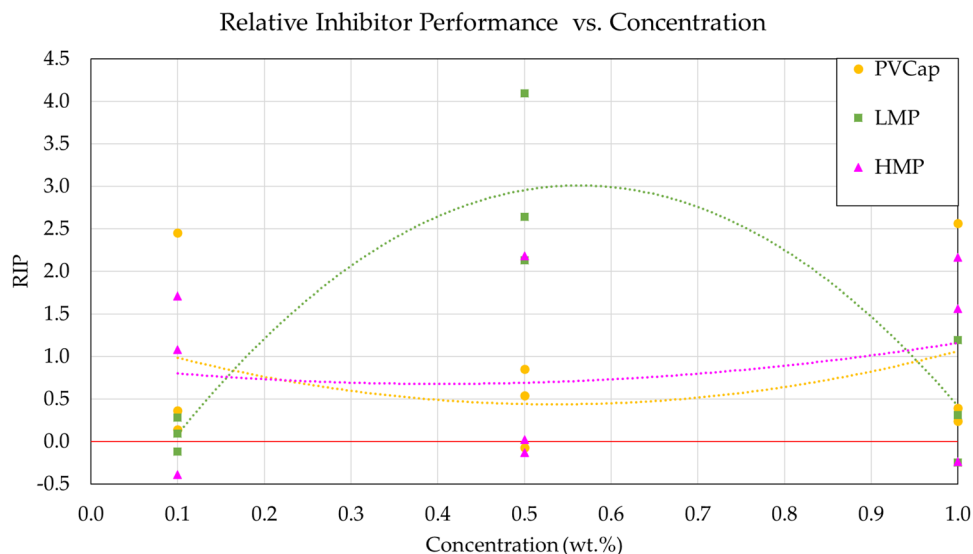


**Fig. 12** Relative inhibitor performance of tested hydrate inhibitors with respect to concentration



adversely affected. It is also interesting to notice that LMP at both concentrations other than optimum, i.e., 0.1 and 1.0wt% LMP, displays strong tendency to promote hydrate formation. At 0.1wt.% LMP, no data were captured above 200 min, whereas 1.0wt% LMP exhibited a few nucleation events broadly spread between 250 and 650 min. Most of the nucleation events for 1.0wt% LMP, however, were captured at times similar to water samples' nucleation time. Considering each peak is represented by a single capillary tube, there is only 15% chance that 1.0wt% LMP may succeed in inhibition and 85% possibility that it may not have any effect at all.

From Figs. 11 and 12, it can be observed that the LMP can perform better with methane gas hydrates. At optimum concentration of 0.5wt%, LMP may be able to inhibit methane hydrates up to three times longer than PVCap, whereas the RIP was calculated to be as high as six times that of PVCap. In comparison with HMP at 0.5wt%, LMP 0.5wt% performed four times better when performance was compared using RIP; however, on average, twice as much induction time was observed with LMP. This is primarily due to higher polarity of the carboxyl functional group, which attracts water molecules and prevents entrapment of gas molecules to form methane clathrate. HMP and PVCap both have higher ratio of hydrophobic functional groups. However, the concentration other than the optimum 0.5wt% concentration significantly reduces the efficacy of LMP. It may be deduced that at lower concentrations LMP is not effective because of the low polar activity of the polymer, whereas at higher concentrations, hyperactivity of these polymers can lead to hydrate promotion. These results agree with previous research conducted on impact of functional group, where higher presence of carboxyl functional group increases the

performance and higher presence of alkyl functional group decreases the performance (Zhang and Kelland 2018). However, key takeaways from this research are that applying this modification to a repeating unit instead of addition of these functional groups as side chains can significantly impact the performance and application of the polymer.

The performance of synthetic (Polycaprolactum) and organic (low- and high-methoxylated pectin) inhibitors on methane hydrate formation and dissociation was tested using HP- $\mu$ DSC. Equilibrium test using capillary tubes proved that more hydrate formation can be observed with higher surface exposure, and with separate samples, more nucleation events can be captured which can reduce the experiment time and cost. However, even without the use of silica gel, experiments conducted still displayed good visibility on hydrate formation and dissociation events due to the increased surface exposure. In total, 12 samples for each inhibitor were done for each of the concentration (36 samples for each inhibitor).

## Conclusion

The kinetic hydrate inhibitor performance test showed that all chemicals were able to delay the onset of hydrate nucleation, with LMP being the most effective at delaying nucleation with optimum concentration of 0.5 wt%. Complex and broad peaks were observed in the presence of synthetic inhibitor, PVCap, especially in the early periods of the test which continued to vary with subsequent repetitions. In contrast, LMP formed few slim peaks but with a wider range in time. Optimum concentration was 0.5wt% for LMP, but it is

also the concentration where the other inhibitors displayed the weakest performance. Although these tests were conducted on a high subcooling of 25 °C, under normal conditions field conditions LMP 0.5 wt% proves a far better solution for mitigation of methane gas hydrates than industrially used polymer, PVCap which agrees with findings from (S. Xu, et al. 2016a, b). However, for HMP, due to its high percentage of ester functional groups, it may be applicable to hydrate inhibition in the presence of CO<sub>2</sub> instead. Therefore, a study using a different gas composition to compare test HMP is suggested. Also, this also informs the importance of functional group present for hydrate inhibition. As pectin

is chemically modifiable (by substitution, hydrolyzation, amidation and chain elongation) that increase its hydrophobicity and hydrophilic behavior, study using modified pectin should be attempted for further research on pectin as a kinetic hydrate inhibitor.

## Appendix

See appendix Figs. 13, 14, 15, 16, 17, 18, 19, 20, 21.

**Fig. 13** Results obtained by using PVCap 0.10 wt%

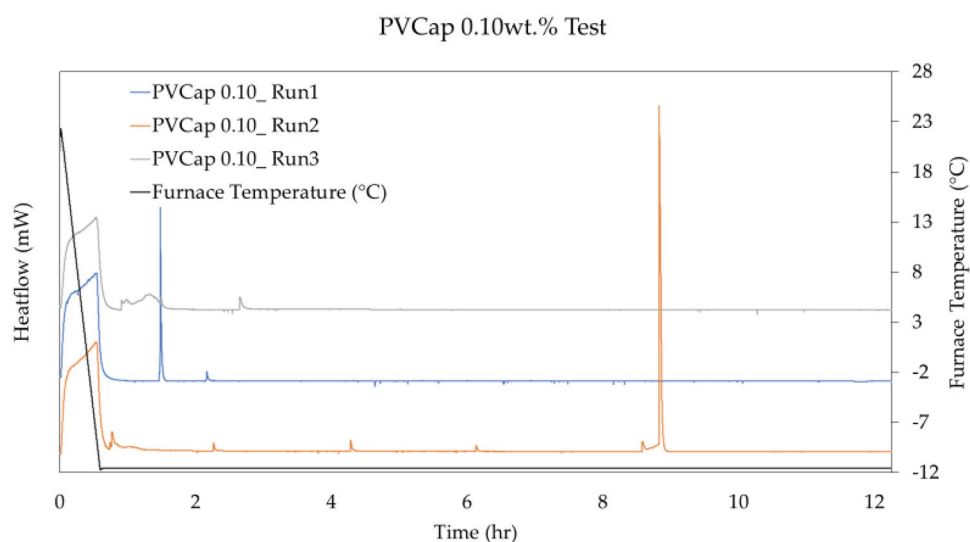


**Fig. 14** Results obtained by using PVCap 0.50 wt%

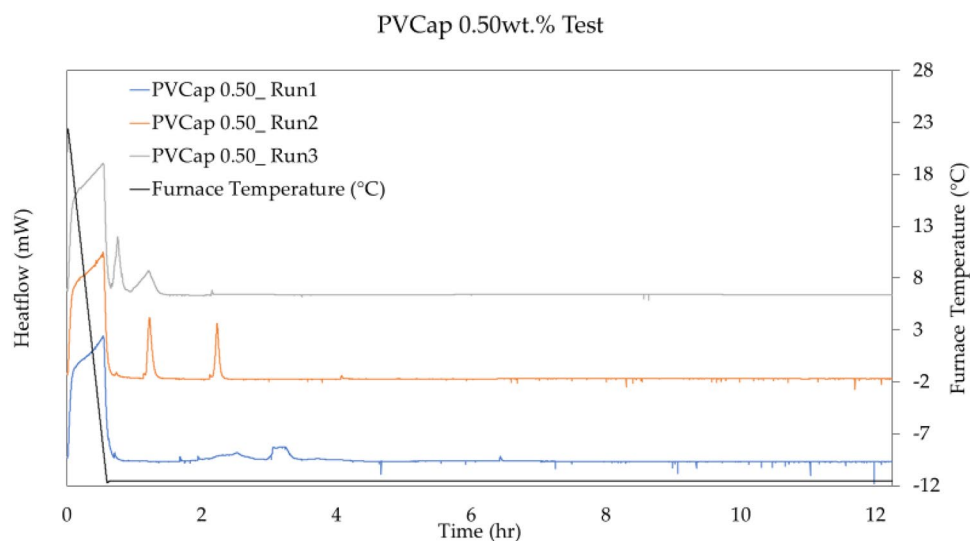


**Fig. 15** Results obtained by using PVCap 1.00 wt%

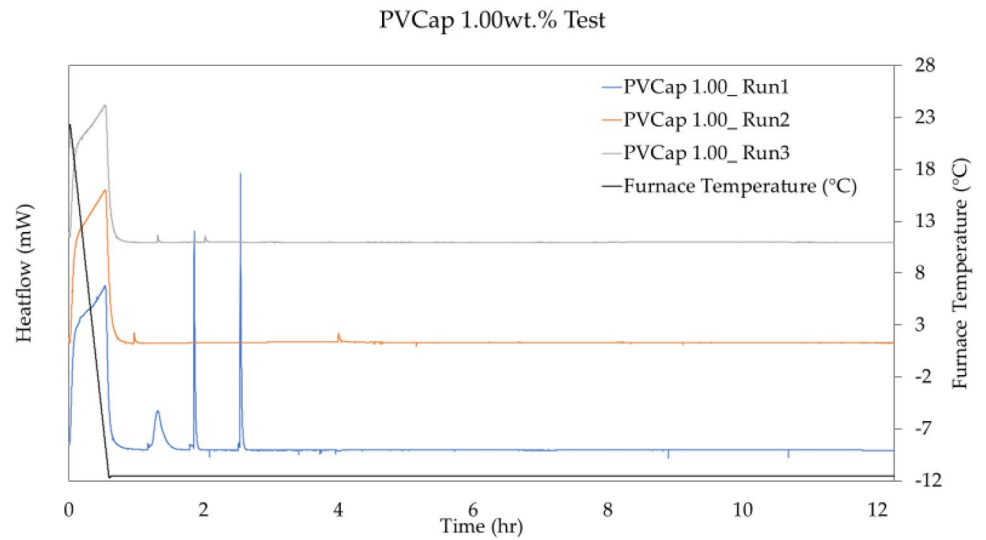


**Fig. 16** Results obtained by using HMP 0.10 wt%

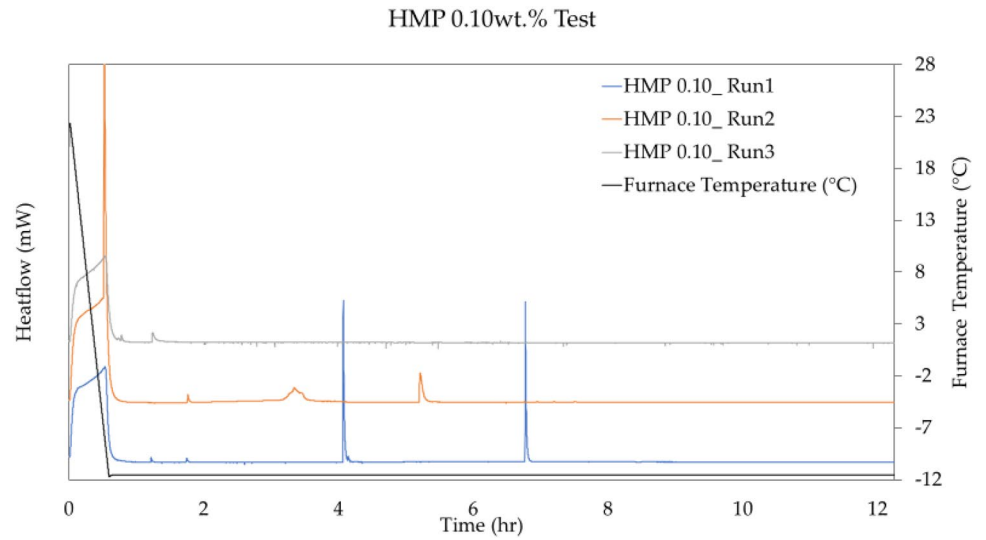


**Fig. 17** Results obtained by using HMP 0.50 wt%

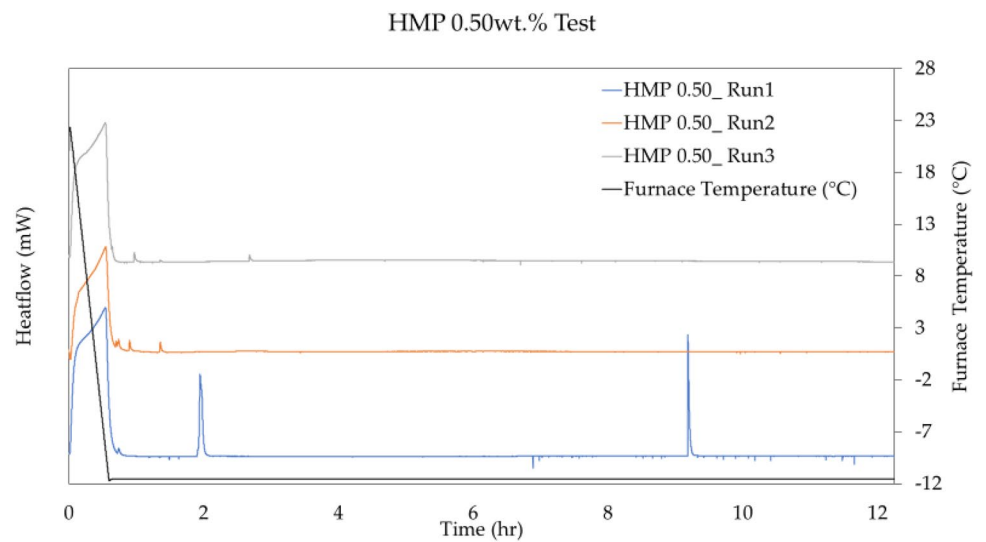


**Fig. 18** Results obtained by using HMP 1.00 wt%

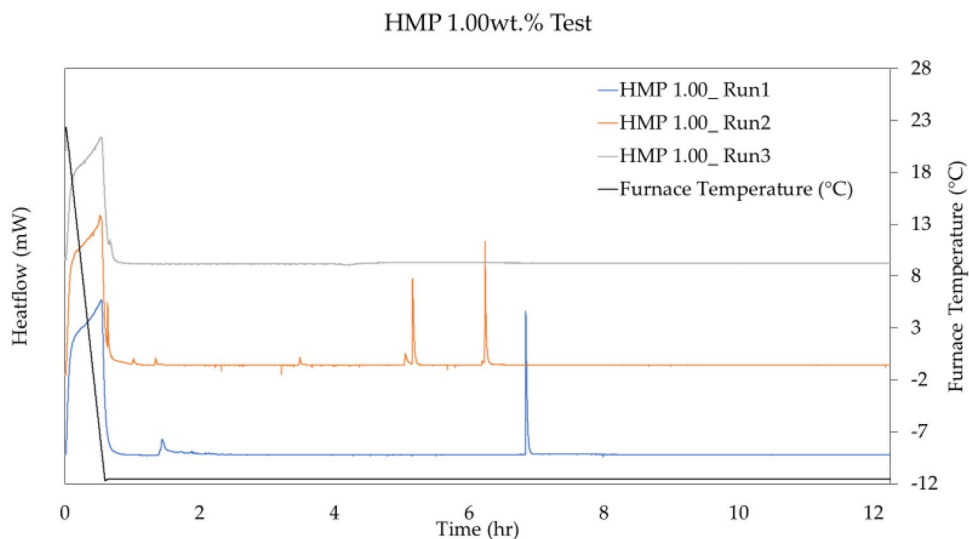


**Fig. 19** Results obtained by using LMP 0.10 wt%

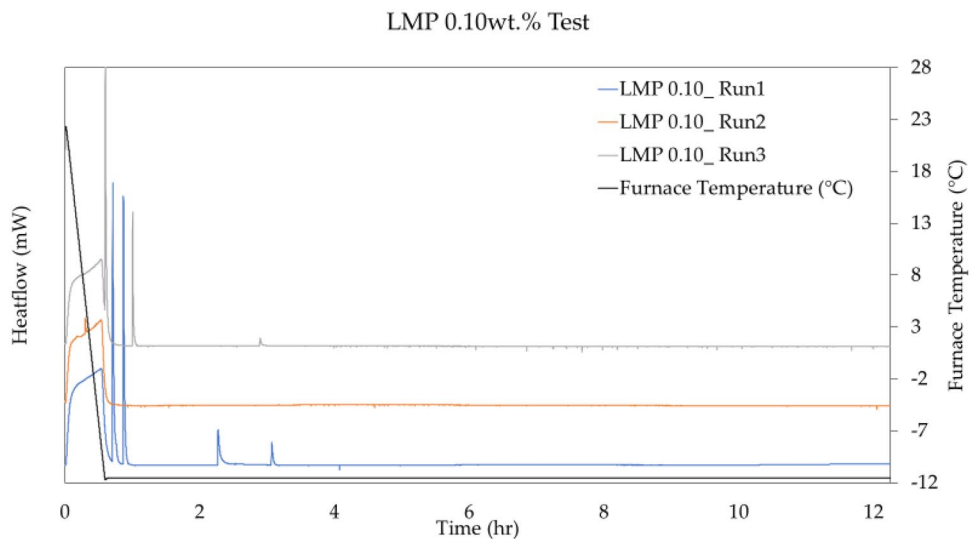


**Fig. 20** Results obtained by using LMP 0.50 wt%

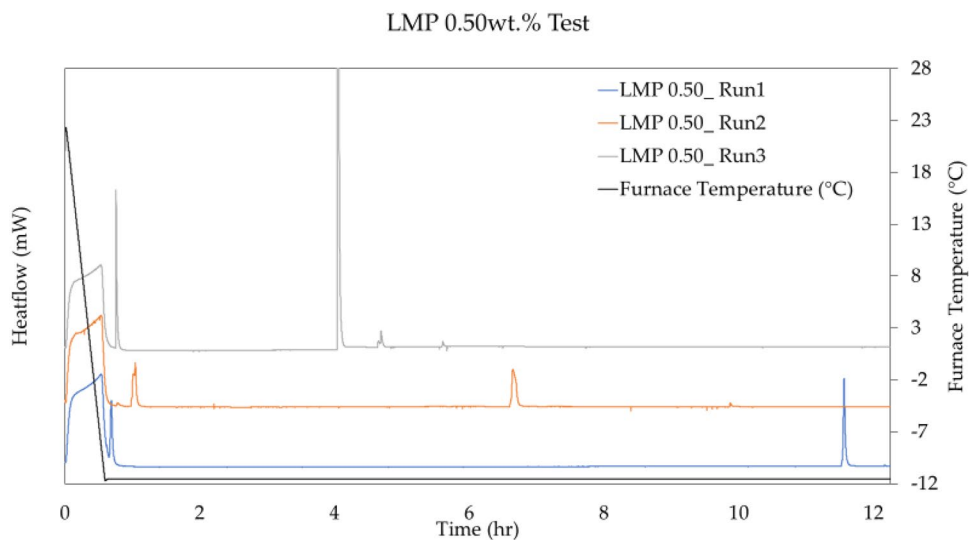
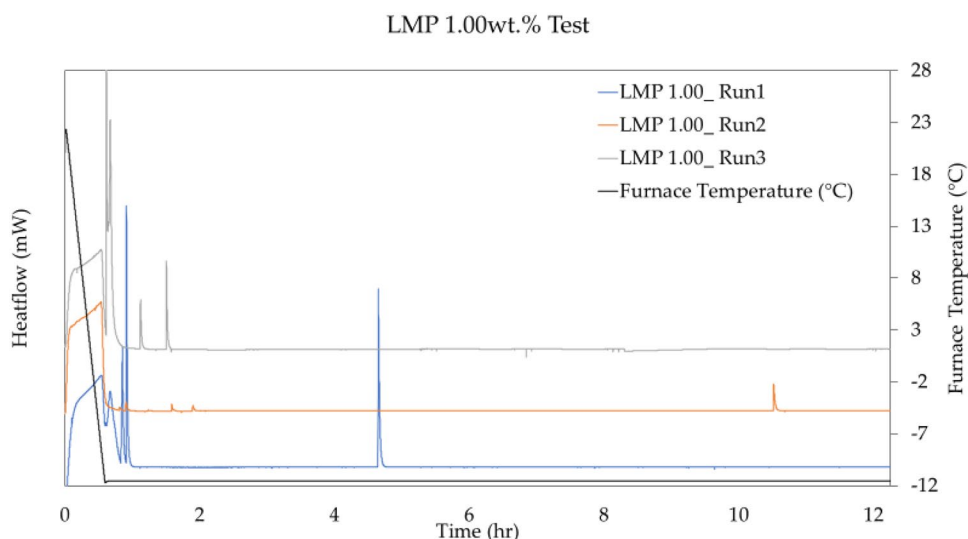


**Fig. 21** Results obtained by using LMP 1.00 wt%



**Acknowledgements** The authors would like to acknowledge Centralized Analytical Laboratory, Universiti Teknologi PETRONAS for the technical assistance with HP- $\mu$ DSC.

**Funding** This research was funded by YAYASAN UNIVERSITI TEKNOLOGI PETRONAS (YUTP), Grant numbers: 015-LC0160 and 015-LC0230.

## Declarations

**Conflict of interest** The authors declare no conflict of interest. The funders had no role in the design of the study; in the collection, analyses, or interpretation of data; in the writing of the manuscript, or in the decision to publish the results.

**Open Access** This article is licensed under a Creative Commons Attribution 4.0 International License, which permits use, sharing, adaptation, distribution and reproduction in any medium or format, as long as you give appropriate credit to the original author(s) and the source, provide a link to the Creative Commons licence, and indicate if changes were made. The images or other third party material in this article are included in the article's Creative Commons licence, unless indicated otherwise in a credit line to the material. If material is not included in the article's Creative Commons licence and your intended use is not permitted by statutory regulation or exceeds the permitted use, you will need to obtain permission directly from the copyright holder. To view a copy of this licence, visit <http://creativecommons.org/licenses/by/4.0/>.

## References

- Baek S, Min J, Ahn Y-H, Cha M, Lee JW (2018) Effect of hydrophobic silica nanoparticles on the kinetics of methane hydrate formation in water-in-oil emulsions. *Energy Fuels* 33(1):523–530
- Chen J, Liu W, Liu C-M, Li Ti, Liang R-H, Luo S-J (2015) Pectin modifications: a review. *Crit Rev Food Sci Nutr* 55(12):1684–1698
- Daraboina N, Ripmeester J, Walker VK, Englezos P (2011) Natural gas hydrate formation and decomposition in the presence of kinetic inhibitors. 1. high pressure calorimetry. *Energy Fuels* 25(10):4392–4397
- Daraboina N, Malmos C, von Solms N (2013) Investigation of kinetic hydrate inhibition using a high pressure micro differential scanning calorimeter. *Energy Fuels* 27(10):5779–5786
- Daraboina N, Perfeldt CM, von Solms N (2015) Testing antifreeze protein from the longhorn beetle *Rhagium mordax* as a kinetic gas hydrate inhibitor using a high-pressure micro differential scanning calorimeter. *Can J Chem* 93(9):1025–1030
- Farhadian A, Varfolomeev MA (2019) The effect of molecular weight of waterborne polyurethanes on kinetic hydrate inhibition. *Int Multidiscip Sci GeoConf: SGEM* 19(12):1109–1115
- Gayet P, Christophe DG, Marion AG, Lachaise J, Nesterov A (2005) Experimental determination of methane hydrate dissociation curve up to 55 MPa by using a small amount of surfactant as hydrate promoter. *Chem Eng Sci* 60(21):5751–5758
- Gupta P, Sangwai J (2017) Non-isothermal Kinetics of Methane Hydrate Formation in Aromatic Based Ionic Liquids: Effect of Carbon Chain Length.
- Idress M, Shahril MA, Zuraidin AS, Jasamai M (2019) Experimental investigation of methane hydrate induction time in the presence of cassava peel as a hydrate inhibitor. *Energies* 12(12):2314
- Jiménez-Ángeles F, Firoozabadi A (2018) Hydrophobic hydration and the effect of NaCl salt in the adsorption of hydrocarbons and surfactants on clathrate hydrates. *ACS Cent Sci* 4(7):820–831
- Kamal MS, Hussein IA, Sultan AS, von Solms N (2016) Application of various water soluble polymers in gas hydrate inhibition. *Renew Sustain Energy Rev* 60:206–225
- Kang SP, Shin JY, Lim JS, Lee S (2014) Experimental measurement of the induction time of natural gas hydrate and its prediction with polymeric kinetic inhibitor. *Chem Eng Sci* 116:817–823
- Kelland MA (2016) *Production chemicals for the oil and gas industry*. CRC Press
- Kelland MA (2018) A review of kinetic hydrate inhibitors from an environmental perspective. *Energy Fuels* 32(12):12001–12012
- Li D, Laroui A, Ma S, Wang J, Wang D, Kelland MA, Dong J (2020) Dependence of the kinetic hydrate inhibition effect of poly (N-vinylpyrrolidone) upon the molecular weight is influenced by water mobility in millisecond dynamics. *Energy Fuels* 34(11):13664–13672
- Liu J, Feng Y, Yan Y, Yan Y, Zhang J (2020) Understanding the inhibition performance of polyvinylcaprolactam and interactions with water molecules. *Chem Phys Lett* 761:138070



- Maeda N, Kelland MA, Wood CD (2018) Ranking of kinetic hydrate inhibitors using a high pressure differential scanning calorimeter. *Chem Eng Sci* 183:30–36
- Makogon TY (2019) Handbook of multiphase flow assurance. Gulf Professional Publishing
- Makwashi N, Zhao D, Ismaila TA, Paiko I (2018) Pipeline gas hydrate formation and treatment: a review. In: 3rd national engineering conference on building the gap between academia and industry, Faculty of Engineering, Bayero University, Kano
- McCain WD (1990) The properties of petroleum fluids. PennWell Publishing Company, Tulsa Oklahoma
- Nashed O, Sabil KM, Ismail L, Jaafar A (2014) Hydrate equilibrium measurement of single CO<sub>2</sub> and CH<sub>4</sub> hydrates using micro DSC. *J Appl Sci* 14(23):3364–3368
- Nguyen NN, Nguyen AV (2017) Hydrophobic effect on gas hydrate formation in the presence of additives. *Energy Fuels* 31(10):10311–10323
- Rogers R (2015) Hydrate inhibition during drilling and production. *Offshore Gas Hydrates* 151–187
- Sayah MY, Chabir R, Benyahia H, Kandri YR, Chahdi FO, Touzani H, Errachidi F (2016) Yield, esterification degree and molecular weight evaluation of pectins isolated from orange and grapefruit peels under different conditions. *PLoS ONE* 11(9):e0161751
- Sa J-H, Kwak G-H, Lee BR, Park D-H, Han K, Lee K-H (2013) Hydrophobic amino acids as a new class of kinetic inhibitors for gas hydrate formation. *Sci Rep* 3(1):1–7
- Sa J-H, Kwak G-H, Lee BR, Ahn D, Lee K-H (2014) Abnormal incorporation of amino acids into the gas hydrate crystal lattice. *Phys Chem Chem Phys* 16(48):26730–26734
- Semenov AP, Medvedev VI, Mikhailov SB, Gushchin PA (2015) Effect of pressure on the effectiveness of the kinetic inhibition of hydrate formation by polymer reagents. *Chem Technol Fuels Oils* 50(6):489–493
- Silva BLLD, Bruna CLD, Silva BOF, JA de C, Teixeira A COBEM-2017–0102 pectin as a biological kinetic inhibitor on the nucleation of gas hydrates
- Sloan ED Jr, Koh CA (2007) Clathrate hydrates of natural gases. CRC press
- Sriamornsak P (2003) Chemistry of pectin and its pharmaceutical uses: a review. *Silpakorn Univ Int J* 3(1–2):206–228
- Tohidi F, Anderson R, Tohidi B (2018) Effect of acid gases on kinetic hydrate inhibitors. *J Chem Thermodyn* 117:119–127
- Vanitha T, Mahejibin K (2019) Role of pectin in food processing and food packaging. Pectins-extraction purification characterization and applications
- Villano D, Luca RK, Kelland MA (2008) Class of kinetic hydrate inhibitors with good biodegradability. *Energy Fuels* 22(5):3143–3149
- Wang Y, Fan S, Lang X (2019) Reviews of gas hydrate inhibitors in gas-dominant pipelines and application of kinetic hydrate inhibitors in China. *Chin J Chem Eng* 27(9):2118–2132
- Xu P, Lang X, Fan S, Wang Y, Chen J (2016a) Molecular dynamics simulation of methane hydrate growth in the presence of the natural product pectin. *J Phys Chem C* 120(10):5392–5397
- Xu Y, Yang M, Yang X (2010) Chitosan as green kinetic inhibitors for gas hydrate formation. *J Nat Gas Chem* 19(4):431–435
- Xu S, Fan S, Fang S, Lang X, Wang Y, Chen J (2016b) Pectin as an extraordinary natural kinetic hydrate inhibitor. *Sci Rep* 6(1):1–7
- Yaqub S, bin Mohd Shariff A, Mellon NB (2019) Unraveling the effect of sub-cooling temperatures on the kinetic performance of biopolymers for methane hydrate. *J Nat Gas Sci Eng* 65:68–81
- Yaqub S, Lal B, Partoon B, Mellon NB (2018) Investigation of the task oriented dual function inhibitors in gas hydrate inhibition: A review. *Fluid Phase Equilib* 477:40–57
- Zhang Q, Kelland MA (2018) Study of the kinetic hydrate inhibitor performance of poly (N-vinylcaprolactam) and poly (N-isopropylmethacrylamide) with varying end caps. *Energy Fuels* 32(9):9211–9219

**Publisher's Note** Springer Nature remains neutral with regard to jurisdictional claims in published maps and institutional affiliations.